euspen's 21st International Conference & Exhibition, Copenhagen, DK, June 2021
www.euspen.eu

Controlling the flank geometry of injection moulded polymer microneedles made with laser ablated moulds by adapting laser scanning parameters

T. Evens[1], P. Vanwersch[1,2], S. Castagne[2], D. Seveno[3], O. Malek[4], A. Van Bael[1,3]

[1] *KU Leuven, Department of Materials Engineering, Diepenbeek Campus, Belgium*
[2] *KU Leuven, Department of Mechanical Engineering and Flanders Make@KU Leuven-MaPS*
[3] *KU Leuven, Department of Materials Engineering, Leuven, Belgium*
[4] *Sirris, Precision Manufacturing , Belgium*

tim.evens@kuleuven.be

Abstract
Microneedle arrays contain minimally invasive devices which facilitate self-administration of drugs in a straightforward and efficient way. In a recent work, we demonstrated a novel methodology to mass produce solid polymer microneedles at a low cost. This production technique utilises a femtosecond laser with a cross-hatching strategy to create cone-shaped micro-holes, which are afterwards replicated using polymer injection moulding. The depth and aspect ratio of the micro-holes can be adapted by changing laser scanning parameters. However, it has not yet been demonstrated how the flank geometry of the needle cavity can be changed. Yet, this flank geometry has a huge impact on both the mechanical strength and the penetration behaviour of the replicated polymer microneedles. In this study, we have modified the flank geometry of laser induced microneedle cavities by adapting laser scanning parameters. This was done by changing the programmed diameter throughout the laser ablation process. Hereby, it was possible to widen the width of a needle near the base to increase its strength and decrease the width near the needle tip of another needle. The laser ablated moulds are replicated through polymer injection moulding, and afterwards the geometry of the resulting microneedles was assessed.

Laser machining; Injection moulding; Microneedles; Micro manufacturing

1. Introduction

Microneedles are micron-sized invasive structures which can be used to deliver vaccines, antibodies or other drugs to the human body through the transdermal route [1–4]. These microneedles are typically arranged in an array and consist of tens to thousands of microneedles per cm². Depending on the application, the individual needle lengths can range from 50 to 2000 µm [5]. The key advantage of microneedles compared to traditional hypodermic needles is their pain-free skin penetration, which is a result of the microneedles not reaching deep enough to stimulate nerve endings [6]. Besides, it is possible to integrate these microneedles on a microfluidic lab-on-a-chip, which facilitates self-administration for patients [7,8]. This process avoids the need of skilled medical personnel and the risk of cross-contamination [9]. Moreover, due to their small volume, costs related to storage and distribution will be much lower compared to traditional needles. However, manufacturing these microneedles in large volumes at a low cost represents a real challenge [6].

Recently, a novel methodology to mass produce solid polymer microneedles at a low cost was developed [10]. First, cone-shaped micro-cavities with very sharp tip radii are ablated in metal mould inserts using a femtosecond laser. These mould inserts are then used in an injection moulding process to create polymer cone-shaped microneedles. The injection moulding process enables the use of different polymer materials, yet it is important that proper injection moulding conditions are used to achieve a good replication fidelity. It is already demonstrated that the depth and base diameter of the microneedles can be changed by adapting the laser scanning parameters [11]. However, it is still not known how the flank geometry of the micro-cavity can be changed, while it is very important for the strength and penetration behaviour of the needles. Sharp needles with small tip radii are needed to effectively pierce the skin at low forces [12,13]. However, the needle design should also take into account the mechanical performance of the needles, to prevent bending or breaking during needle insertion [14,15].

In this study, an existing laser scanning strategy is adapted in order to modify the flank geometry of laser induced microneedle cavities. This is done by changing the programmed base diameter throughout the laser ablation process. Three different microneedle designs are created in a tool steel mould insert. The geometry of the micro-cavities are assessed using micro-computed tomography (µ-CT) and are used in an injection moulding process to create polycarbonate microneedles. Afterwards, the replication fidelity and microneedle geometry are evaluated.

2. Materials and methods

2.1. Materials

The thermoplastic material used in this study is polycarbonate (PC, Lexan™ HPX8REU, manufactured by SABIC). The material is a biocompatible amorphous grade, suitable for medical devices and pharmaceutical applications. The melt flow rate is 35 g/10min, which indicates a high flowability.

The selected mould material is a low corrosion tool steel "Stavax" (grade 1.2083 - AISI 420), which is a common mould material within polymer injection moulding. It is often used for its high wear and corrosion resistance, both leading to a long lifetime.

2.2. Laser machining experiments

A micromachining system (Lasea, Liège, Belgium) with a Satsuma HP femtosecond laser source (Amplitude, Pessac, France) is employed to laser ablate a mould insert with dimensions 70 mm x 60 mm x 4.4 mm. The laser source emits a beam with a pulse duration of 250 fs, a wavelength of 1030 nm and a pulse repetition rate of 500 kHz. The maximum average power of the laser is 7.85 W, giving a deliverable pulse energy of 15.7 µJ. A galvanometer steers the laser beam within the focal plane, with a spot size of 15.0 µm and an average pulse fluence of 8.88 J/cm². Small dust particles which are formed from ablating the metal surface are extracted by a vacuum collect unit.

A cross-hatching laser scanning strategy, which was recently developed [10], is used in this study for the creation of the microneedle cavities. In this strategy, the laser spot is scanned in a circular region and follows parallel lines in two perpendicular directions. The distance between two consecutive lines is defined as the hatch pitch. Once the laser has scanned one circular grid, the focal point is lowered with a vertical distance, defined as the layer pitch, and the laser scans again the same area. This process is repeated multiple times for a prescribed number of layers.

In this study, we created three different designs, each having a different scanning strategy as illustrated in Figure 1. The first design acts as a reference, as this is created by the conventional laser scanning strategy. Here we scanned a circular region with a constant diameter of 400 µm during a total of 300 layers. In the second design we intend to widen the base of the microneedle by adapting the programmed diameter through the laser ablation process. First, a larger circular region with a diameter of 500 µm was scanned during 10 layers. Afterwards, the size of this feature was decreased to a diameter of 450 µm and was scanned during 25 layers. At last, we decreased the diameter to the reference diameter of 400 µm and this region was scanned for 265 layers. Similar to design 1, the total number of layers corresponds to 300. In the third design we aim to decrease the diameter of the needle throughout its height. In this scanning strategy, the programmed diameter was decreased in four steps of 50 µm, starting from the reference diameter of 400 µm. During each of these steps, the circular feature was scanned for 60 layers, creating again a total of 300 layers. For each of the designs, we created a 2x2 array of micro-cavities with an interspacing between the cavities of 1 mm. The hatch pitch, layer pitch and scanning speed were constant throughout all of the experiments being 15 µm, 2 µm and 100 mm/s respectively.

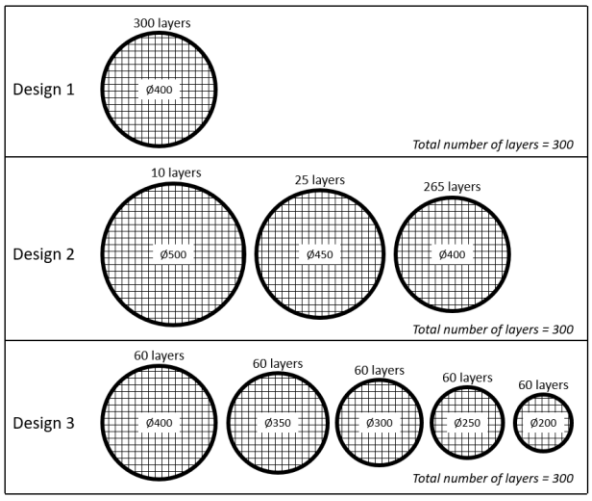

Figure 1. Three different laser scanning designs, each having a different programmed diameter throughout the laser ablation process.

2.3. Replication through injection moulding

Injection moulding was done on an Engel ES 200/35 HL hydraulic injection moulding machine (Engel, Schwertberg, Austria) with a maximum clamping force of 350 kN and a 25 mm screw with an L/D ratio of 24.8. The mould temperature is controlled by a WITTMANN TEMPRO Controller (Wittmann, Vienna, Austria). The injection moulded part is a 50 mm x 60 mm x 1.5 mm flat plate. Injection moulding parameters are given in Table 1 and were defined to achieve a high replication fidelity. The injection temperature was set to the recommended upper limit of the material supplier. The mould temperature was set to a high value to delay the formation of the frozen layer during injection. The volumetric injection rate was set to a high value, to increase shear stresses and thus reduce the melt viscosity during injection. The implemented holding pressure was set to a value just below the occurrence of flash. The parts produced in the first 30 cycles were discarded in order to stabilize the process, then the following parts were collected for characterization.

Table 1. Process parameters for injection moulding

	PC
Injection temperature/°C	315
Volumetric injection rate/$cm^3.s^{-1}$	149
Holding pressure/Bar	749
Mould temperature/°C	115

2.4. Topography characterization

The geometries of the ablated microneedle cavities were characterized using a Phoenix Nanotom µ-CT system (Universal Systems, Solon, USA). The device is equipped with a high-power nanofocus X-ray tube and a diamond-tungsten target was chosen for the high X-ray absorbing steel samples. A high-power mode was used to allow focal spot and voxel sizes in the micrometre range. The mould insert was cut into cubic samples with an edge length of approximately 3 mm, using a metallographic precision saw. The cubic samples were mounted on a sample holder and fixed on a high-accuracy computer controlled rotation stage. For each scan, 2400 X-ray 2D projection images were obtained from incremental rotation of the scanned samples over 360°. Acquisition parameters were fixed for all samples as follows: voltage = 100 kV, current = 158 A, voxel size = 3.75 µm, and a 0.1 mm copper and 0.1 mm aluminium filter was used during scanning. Reconstruction of the acquired 2D projections into 3D volumes was performed using GE Phoenix datos|x REC software. Reconstructed datasets (XY-slices) were exported from the software for further analysis and visualization within Fiji ImageJ. For each set of laser parameters, one cubic sample containing four micro-holes were measured. The average length and diameter of the four micro-cavities, along with the standard deviation was reported in the results.

The geometry of the replicated thermoplastic microneedles were assessed using a Keyence VH-S30 digital microscope (Keyence, Osaka, Japan) with a maximum magnification of X200. The system is connected to a VHX-500F monitor with built-in measuring software. Ten injection moulded samples were collected and on each sample one microneedle was measured. The average of these ten measurements along with the standard deviation was reported in the results.

3. Results

3.1. Laser ablation

The reconstructed µ-CT XY datasets of the laser ablated microneedle designs with corresponding dimensions are shown in Figure 2. First of all, we can clearly observe cone-shaped micro-cavities with very sharp tip radii for each of the three designs. The formation of this cone-shape is expected to be caused by two laser phenomena, being plasma shielding and laser reflectance on steep sidewalls. Plasma shielding occurs at a laser ablation process with high repetition rates [16]. A part of the vaporized material which is formed during the ablation process will be unable to escape for the micro-cavity. Therefore, it will interact with the next incoming laser pulse, creating a protective plasma shield [17]. Secondly, the ablation efficiency of the laser is reduced drastically near the edge of the cavity, as most of the laser light is reflected rather than absorbed. This causes the diameter of the micro-cavity to become smaller as the micro-hole is created [18]. Furthermore, the reflected laser light will partially be redirected to the bottom of the hole, contributing to a deeper and sharper cavity.

When comparing the three different needle designs, we can observe a difference in cavity dimensions. The base diameter of design 2 (500 ± 3 µm) is higher compared to the diameter of reference design 1 (437 ± 2 µm). The diameter of design 2 is only wider near the base of the needle and gradually changes to a comparable shape of design 1. Moreover, it can be seen that the length of both cavities is also the same. Thus, by increasing the size of the scanned circular feature during the first few layers, the base of the cavity is increased while the rest of the needle shape stays similar to the reference.

In design 3, the diameter is decreased four times throughout the laser scanning process. This results in a micro cavity which gradually reduces in diameter throughout the depth, compared to reference design 1. Thus, the needle has a sharper shape compared to design 1. Besides, the cavity base diameter is smaller than reference design 1 and can be explained as followed. During the laser ablation process, the laser focal spot is progressively moved deeper inside the mould material. Therefore, the Gaussian shaped laser beam will start to intersect with the edge of the already created micro-hole, removing additional material. As a result, we can observe that the base diameter of design 1 (437 µm) is larger than the programmed base diameter (400 ± 2 µm). However, for design 3, the scanned diameter is progressively decreased in size, preventing the laser beam to be in contact with the existing micro-hole. Thus, here the size of the base diameter (406 ± 3 µm) is almost identical to the programmed base diameter (400 µm).

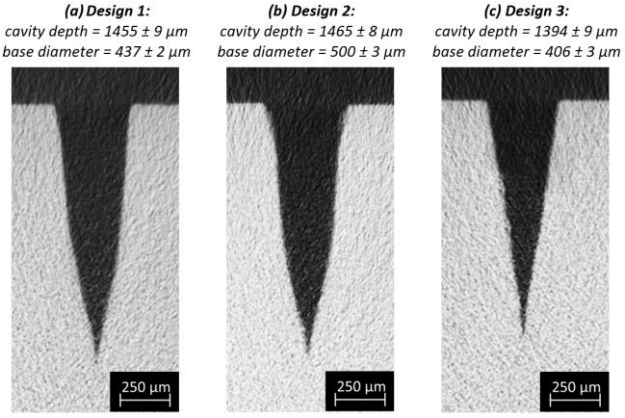

Figure 2. Reconstructed µ-CT XY datasets of the ablated micro-cavities for: (a) design 1; (b) design 2, and (c) design 3.

3.2. Injection moulding

The laser ablated mould insert was used in an injection moulding process to replicate the microneedle cavities. The replicated polymer microneedles together with the needle length and replication in height are shown in Figure 3. All of the microneedles show a similar shape as the corresponding microneedle cavity. Yet, the tip of the polymer microneedles are not completely replicated.

Completely filling micro-cavities is known to be very difficult within polymer injection moulding [19]. When the polymer is injected into the mould, it will follow the path of least resistance. Therefore, most of the material will flow in the main flow direction through the macroscale cavity, leaving the micro-features only partially filled. This behaviour is also known as the hesitation effect [20]. Yet, as soon as the polymer comes in contact with the cold mould surface, a layer of frozen polymer is formed which will prevent the complete filling if the micro-cavities at the time when the macroscale cavity is filled and the pressure is built up. This behaviour is in our case minimized, by increasing the mould temperature which delays the formation of the frozen polymer layer. Therefore, a relatively high replication fidelity can be observed for all three designs. The needles replicated for design 1 and design 2 exhibit a very similar replication in height, being 91 % and 92 %, respectively. The lowest replication was observed for design 3, which corresponded to 86 ± 0.9 %.

The reason why the replication of design 3 is lower compared to the other two designs is due to the difference in the shape of the needle cavity. The micro-cavity of design 3 is much sharper near the needle tip, which increases both the filling resistance of the polymer and the surface area to volume ratio. As a result of the latter, the heat transfer between the molten polymer and the mould surface is higher [21]. This causes a faster solidification of the polymer leading to a faster formation of the frozen layer and in turn a lower replication fidelity.

It is evident that the performance of the three different microneedle designs will be different in terms of mechanical strength and skin penetration behaviour, due to the difference in needle shape. In design 2, a curvature is added to the base of the microneedle. It is expected that this curvature will not affect the insertion behaviour of the needle tip, yet an increase in the penetration force is likely when the whole needle would be completely forced into the skin. Yet, the additional curvature will reduce stress concentrations at the base of the needle and will improve the mechanical performance of the microneedle. The design of needle 3 is expected to reduce the force needed to penetrate the microneedle into the skin, due to the sharper shape of the needle.

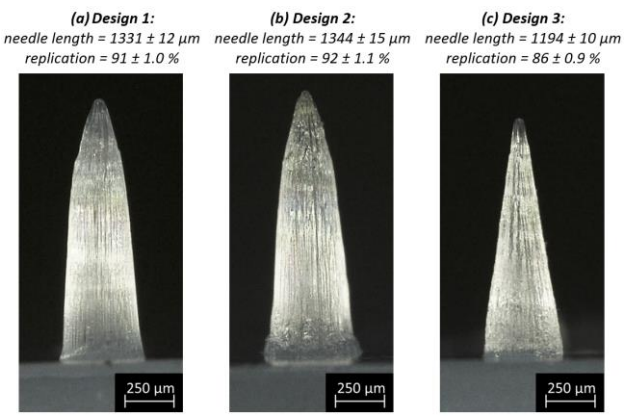

Figure 3. Microscopic images of the polymer microneedles corresponding to: (a) design 1, (b) design 2, and (c) design 3.

4. Conclusion

In this study, we have shown that it is possible to adapt the flank geometry of laser induced micro-cavities, by adapting laser scanning parameters. We created three different designs, each having a different scanning strategy. The first design acted as a reference, as it was created by the conventional strategy, which has a constant programmed diameter throughout the scanning process. In the second design we increased the width of the cavity near the surface, by increasing the programmed diameter in the first few layers. In the third design we created a micro-cavity with a sharp flank geometry compared to the reference design. This was done by decreasing the programmed diameter throughout the number of layers. The ablated micro-cavities were assessed by μ-CT and were used in an injection moulding process to create polycarbonate microneedles. A relatively high replication fidelity was observed for all of the three designs, being 91 %, 92 % and 86 %, for design 1, design 2 and design 3, respectively. Design 3 exhibited the lowest replication fidelity, which was caused by its sharper needle geometry. Evidently, the performance of the three different microneedle designs will be different in terms of mechanical strength and skin penetration behaviour, due to the difference in needle shape.

In future work, a model will be developed to simulate the laser ablation process. With the aid of this model, we will further optimise the geometry of the microneedle to improve its mechanical strength and penetration behaviour. This will be done in combination with micro-mechanical finite element analyses. In addition, micromechanical testing equipment will be developed to quantify this needle strength and penetration behaviour. Furthermore, an in-depth analysis on the replication fidelity during the injection moulding process will be conducted.

Funding

This work was funded by the KU Leuven Interdisciplinary Network project IDN/20/011 - MIRACLE: Autonomous microfluidic patch for plasmid-based vaccine.

Acknowledgements

The authors would like to thank the company SABIC for providing the Lexan™ HPX8REU polycarbonate resin.

References

[1] Juster H, van der Aar B, de Brouwer H 2019 A review on microfabrication of thermoplastic polymer-based microneedle arrays *Polym Eng Sci*. **59** 877–90. https://doi.org/10.1002/pen.25078.

[2] Donnelly RF, Singh TRR, Morrow DIJ, Woolfson AD 2012 *Microneedle-mediated Transdermal and Intradermal Drug Delivery* (Pondicherry)

[3] Tucak A, Sirbubalo M, Hindija L, Rahić O, Hadžiabdić J, Muhamedagić K, et al. 2020 Microneedles: Characteristics, materials, production methods and commercial development *Micromachines* **11**

[4] Ceyssens F, Chaudhri BP, Van Hoof C, Puers R. 2013 Fabrication process for tall, sharp, hollow, high aspect ratio polymer microneedles on a platform. J Micromechanics *Microengineering* **23**.

[5] Li X (James), Zhou Y. 2013 *Microfluidic devices for biomedical applications* (Woodhead Publ. Ser. Biomater. Cambridge: Woodhead Publishing Limited) p. 1–652.

[6] Larrañeta E, Lutton REM, Woolfson AD, Donnelly RF 2016 Microneedle arrays as transdermal and intradermal drug delivery systems: Materials science, manufacture and commercial development. *Mater Sci Eng R Reports* **104** 1–32

[7] Attia UM, Marson S, Alcock JR. 2009 Micro-injection moulding of polymer microfluidic devices. *Microfluid Nanofluidics* **7** 1–28

[8] Indermun S, Luttge R, Choonara YE, Kumar P, Du Toit LC, Modi G, et al. 2014 Current advances in the fabrication of microneedles for transdermal delivery *J Control Release* **185** 130–138

[9] Wang QL, Zhu DD, Chen Y, Guo XD. 2016 A fabrication method of microneedle molds with controlled microstructures. *Mater Sci Eng C* **65** 135–142

[10] Evens T, Malek O, Castagne S, Seveno D, Van Bael A. 2020 A novel method for producing solid polymer microneedles using laser ablated moulds in an injection moulding process. *Manuf Lett* **24** 29–32

[11] Evens T, Malek O, Castagne S, Seveno D, Van Bael A. 2021 Controlling the geometry of laser ablated microneedle cavities in different mould materials and assessing the replication fidelity within polymer injection moulding. *J Manuf Process* **62** 535–545

[12] Bodhale DW, Nisar A, Afzulpurkar N. 2010 Structural and microfluidic analysis of hollow side-open polymeric microneedles for transdermal drug delivery applications. *Microfluid Nanofluidics* **8** 373–92.

[13] Luttge R, Berenschot EJW, de Boer MJ, Altpeter DM, Vrouwe EX, van den Berg A, et al. 2007 Integrated lithographic molding for microneedle-based devices. *J Microelectromechanical Syst* **16** 872–884

[14] Larrañeta E, Lutton REM, Woolfson a D, Donnelly RF. 2016 Microneedle arrays as transdermal and intradermal drug delivery systems: Materials science, manufacture and commercial development. *Mater Sci Eng R Reports* **104** 1–32.

[15] Uppuluri CT, Devineni J, Han T, Nayak A, Nair KJ, Whiteside BR, et al. 2017 Microneedle-assisted transdermal delivery of Zolmitriptan: effect of microneedle geometry, in vitro permeation experiments, scaling analyses and numerical simulations. *Drug Dev Ind Pharm* **43** 1292–1303.

[16] Cheng J, Perrie W, Edwardson SP, Fearon E, Dearden G, Watkins KG. 2009 Effects of laser operating parameters on metals micromachining with ultrafast lasers. *Appl Surf Sci* **256** 1514–1520.

[17] Bulgakov A V, Bulgakova NM 1999 Thermal model of pulsed laser ablation under the conditions of formation and heating of a radiation-absorbing plasma. *Quantum Electron* **29** 433–437.

[18] Audouard E, Mottay E. 2016 Engineering model for ultrafast laser microprocessing. *Front Ultrafast Opt Biomed Sci Ind Appl XVI* **9740** 1-15

[19] Tosello G 2018 *Micro Injection Molding* (München: Carl Hanser Verlag GmbH & Co. KG); 2018.

[20] Masato D, Sorgato M, Lucchetta G. 2017 Characterization of the micro injection-compression molding process for the replication of high aspect ratio micro-structured surfaces *Microsyst Technol* **23** 3661–3670.

[21] Hill SDJ, Kämper KP, Dasbach U, Döpper J, Erhfeld W, Kaupert M. 1995 An investigation of computer modelling for micro-injection moulding. *Proc Microsym'95* **12** 275–283.